Physica Medica 57 (2019) 153–159

Contents lists available at ScienceDirect

Physica Medica

journal homepage: www.elsevier.com/locate/ejmp

Technical note

Partial volume effect of SPECT images in PRRT with 177Lu labelled somatostatin analogues: A practical solution

Domenico Finocchiaro[a,b], Salvatore Berenato[c], Elisa Grassi[a,*], Valentina Bertolini[a], Gastone Castellani[b], Nico Lanconelli[b], Annibale Versari[d], Emiliano Spezi[c,e], Mauro Iori[a], Federica Fioroni[a]

[a] Azienda Unità Sanitaria Locale – IRCCS di Reggio Emilia, Medical Physics Unit, Reggio Emilia, Italy
[b] Department of Physics, University of Bologna, Italy
[c] School of Engineering, Cardiff University, Cardiff, UK
[d] Azienda Unità Sanitaria Locale – IRCCS di Reggio Emilia, Nuclear Medicine Unit, Reggio Emilia, Italy
[e] Department of Medical Physics, Velindre Cancer Centre, Cardiff, UK

ARTICLE INFO

Keywords:
Partial volume effect
Partial volume correction
SPECT
Quantitative imaging
Recovery coefficient

ABSTRACT

Background: At present activity quantification is one of the most critical step in dosimetry calculation, and Partial Volume Effect (PVE) one of the most important source of error. In recent years models based upon phantoms that incorporate hot spheres have been used to establish recovery models. In this context the goal of this study was to point out the most critical issues related to PVE and to establish a model closer to a biological imaging environment.

Methods: Two different phantoms, filled with a ^{177}Lu solution, were used to obtain the PVE Recovery Coefficients (RCs): a phantom with spherical inserts and a phantom with organ-shaped inserts. Two additional phantoms with inserts of various geometrical shapes and an anthropomorphic phantom were acquired to compare the real activities to predicted values after PVE correction.

Results: The RCs versus volume of the inserts produced two different curves, one for the spheres and one for the organs. After PVE correction, accuracy on activity quantification averaged over all inserts of three test phantoms passed from −26% to 1.3% (from 26% to 10% for absolute values).

Conclusion: RCs is a simple method for PVE correction easily applicable in clinical routine. The use of two different models for organs and lesions has permitted to closely mimic the situation in a living subject. A marked improvement in the quantification of activity was observed when PVE correction was adopted, even if further investigations should be performed for more accurate models of PVE corrections.

1. Introduction

The quantitative assessment of radioactivity distribution is a critical step in Molecular Radionuclide Therapies (MRT), both for planning and for monitoring of the treatment. Multimodal techniques have permitted to produce quantitative and accurate measurements of tracer concentrations in vivo, and nowadays functional imaging has become a clinical reality [1,2]. Multiple SPECT/CT scans especially allow to derive patient specific pharmacokinetics for dosimetry purpose in MRT [3] in accordance with a simple planar, hybrid, tridimensional or voxelized method [4]. In this scenario deformable image registration algorithms applied to multimodal images help to correct the registration errors derived from misalignment of sequential scans, changes in patient repositioning, organ deformation and respiratory motion [5]. Also optimization of data acquisition and data processing as reported in MIRD No. 24 [6] and in No. 26 [3] for specific MRT techniques have greatly reduced biases in quantifications, as previously hypothesized in MIRD No. 16 [7]. However, the finite spatial resolution of imaging system and the image sampling remain inherent limits in nuclear medicine imaging and still cause a displacement of counts between different image regions: the so called Partial Volume Effect (PVE). This effect is often viewed as two separate effects: spill-in and spill-out, which makes sense when focusing on a volume of interest (VOI) in which the activity needs to be quantified. Adjacent regions are then considered as background regions and are taken into consideration only for their relation with the VOI. PVE is not routinely dealt with in

* Corresponding author.
E-mail address: elisa.grassi@ausl.re.it (E. Grassi).

https://doi.org/10.1016/j.ejmp.2018.12.029
Received 29 June 2018; Received in revised form 26 November 2018; Accepted 20 December 2018
Available online 08 January 2019

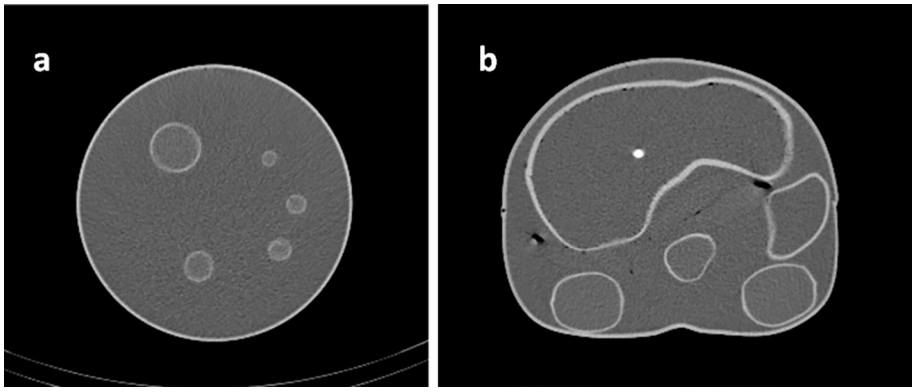

Fig. 1. Axial CT slice of the Sphere phantom (a) and Anthropomorphic phantom (b).

clinical practice, but it is of foremost importance in the context of imaging activity quantification [8].

PVE depends on numerous parameters [9] and it has a very strong dependence on the size of the structure contoured [10]. Different VOIs with exactly the same activity but different sizes yield images with different degree of intensity. Furthermore, correlation between PVE and size of VOI is not linear. Another parameter that influences the PVE is the shape of the structure, and in particular how much 'compact' it is [11]. The term 'compact' refers to the ratio between the surface area and the volume for a given VOI. The larger the ratio, the less compact the VOI. Spherical volumes are the most compact, so they are less affected by the PVE. Instead, in less compact structures a larger part of the inner points is close to the edges and is thus susceptible to spilling in and spilling out. Then PVE depends on the background of surrounding tissue activity, which determines the effect of spilling-in. Finally the spatial resolution of the reconstructed images is also important. This determines how much the signal spreads out around the actual position [12].

One approach to compensate for PVE is to apply Recovery Coefficients (RCs) that have been derived from empirical measurements. These measurements are often performed using phantoms with simple geometries, such as spherical or cylindrical. RC is defined as the ratio of measured activity to true activity in the object. In other words, RC is a factor by which the activity in the VOI is shifted due to PVE.

The aim of this work is to point out the most critical issues related to PVE in SPECT images of ^{177}Lu DOTATOC and to establish a recovery model to correct the number of counts in ^{177}Lu SPECT images. To this end a model based upon phantoms that simulate a clinical context was used, similarly to the partial volume correction implemented for PET recovery calculation [13].

2. Materials and methods

2.1. Image acquisition and reconstruction

All activity measurements were performed with an accurate activity calibrator (Aktivimeter Isomed 1010, Nuklear Medizintechnik, Germany) and all images acquisitions through a SPECT-CT scanner (Symbia T2, Siemens Medical, Germany, 3/8″ NaI(Tl)-detector). The energy windows (EW) of ^{177}Lu photopeaks were set at 113 keV ± 7.5% and 208.4 keV ± 7.5%. For the lower EW, the TEW scatter correction [14] was employed (lower scatter window 87.58–104.53 keV, weight = 0.9375). For the higher EW, the DEW scatter correction [15] was employed (lower scatter window 171.60–192.40 keV, weight = 0.75). The standard clinical protocol for body studies was used: MEHR collimators; matrix 128 × 128; zoom = 1; views = 32 × 2; time/view = 30 s; step and shoot mode; degree of rotation = 180°; non-circular orbit; detector configuration = 180°. The CT acquisition was performed with the following parameters: 130 kV and max = 90 mAs using tube current modulation. The reconstructed slice thickness was 5 mm and a smooth reconstruction kernel was used (B08s; Siemens Medical Solution, Germany).

The SPECT projections were reconstructed by an iterative algorithm with compensations for attenuation from CT images, scatter and full collimator-detector response in Siemens E-Soft workstation (Syngo, MI Application version 32B, Siemens Medical Solution, Germany) with Flash 3D iterative algorithm (10 iterations; 8 subsets; Gaussian filter cut-off = 4.8 mm; 4.8 mm cubic voxel) [16].

For quantitative imaging, a partial volume free calibration factor (CF) was previously determined with a cylindrical Jaszczak phantom filled with a homogeneous radioactive solution and considering the activity to counts ratio in the phantom (CF = 28.5 Bq/counts). To avoid PVE, a cylindrical VOI with a radius equal to the reconstructed SPECT image FOV size was used. Once calibrated, counts-to-activity conversion was performed by applying the following formula:

$$\textit{Measured activity} = \textit{CF}\cdot\textit{Counts} \quad (1)$$

The Volume Of Interest (VOI) for each insert was drawn on the CT image by using the contouring toolkit of Velocity 3.2.0 (Varian Medical Systems, Palo Alto, USA). The VOI definition was completely manual, as also suggested by Uribe et al [17]. The VOIs were transferred onto the SPECT voxel grid using the platform CERR [18]. CERR performs a linear interpolation between CT and SPECT coordinates to select SPECT voxels to include into each VOI.

2.2. PHASE 1: Determination of the recovery Coefficients (RCs)

Phantoms were filled with ^{177}Lu in a solution of water and HCl. HCl was used in order to guarantee a homogenous radionuclide solution.

Two different phantoms were used to determine RCs:

1. The Sphere phantom (Jaszczak type phantom, Data spectrum corporation, USA) to mimic isotropic activity distribution (Fig. 1a). This phantom consisted of a cylindrical phantom filled with a radionuclide solution, in which seven spheres and two ellipsoidal inserts with increasing volume were placed. These inserts were filled with the same activity concentration.
2. An anthropomorphic phantom (Liqui-Phill, The Phantom Laboratory; Greenwich, NY) to mimic organ-shape activity distribution (Fig. 1b). This phantom consisted of a human body phantom with organ-shaped inserts (liver, spleen, pancreas and kidney). These organ inserts were hand-designed to be as close as possible to real ones. Each organ was filled with a specific activity concentration and placed in a radioactive solution. The activity concentrations were chosen as close as possible to clinical cases, considering a range of concentrations of each organ in a group of patients.

Table 1
Description of phantoms used to study RCs. Each sphere was named as his diameter (for example the sphere with 10 mm of diameter as Sphere10).

Phantom	Phantom volume (ml)	Insert name	Insert inner Volume (ml)	Background activity concentration (MBq/ml)	Insert activity concentration (MBq/ml)
Sphere phantom	4225	Sphere10	0.6	0.032	0.905
		Sphere13	1.2		
		Sphere17	2.6		
		Sphere22	5.7		
		Sphere28	11.6		
		Sphere37	26.8		
		Sphere57	98.6		
		Falcon48a	58.5		
		Falcon48b	58.9		
Anthropomorphic phantom 1	8153	Pancreas	92	0.0035	0.12
		Right Kidney	142		0.10
		Left Kidney	142		0.10
		Spleen	156		0.14
		Liver	1470		0.07

A description of inserts, volumes and activity concentrations are collected in Table 1. The volume of each phantom was estimated by drawing the contour on the CT image, while the volume of the inserts was derived measuring the weight of the insert before and after the refilling with a calibrated scale (assuming the concentration of the radioactive water is 1 g/ml).

RC was obtained using the following expression [19]:

$$RC = \frac{Measured\ activity}{True\ activity} \quad (2)$$

The Measured activity was obtained using Eq. (1), where CF was previously calculated and Counts were detected in a VOI precisely following the contours of the object in the CT image. The True activity was measured during the preparation of the phantom with the activity calibrator. Uncertainty of the RC value was estimated using the error propagation formula from Measured activity and True activity. Inaccuracy associated to Measured activity was estimated, from a previous study [20], to be 10%. Inaccuracy of True activity was 5%, as reported by the user manual of the activity calibrator.

Once RC is known (Eq. (2)), partial volume corrected activity in VOI can be derived rescaling the Measured activity as summarized with Eq. (3):

$$PVC\ acivity = \frac{Measured\ activity}{RC} = CF/RC{\cdot}Counts \quad (3)$$

2.3. PHASE 2: Assessment of partial volume correction with RCs

To examine the effect of PVC on the quantitative accuracy, two different phantoms were acquired:

1. A cylindrical phantom and a set of 11 different inserts were arranged in two different configurations, to originate two 'Geometrical phantoms'. The inserts, different for shape (toroidal, pear-shaped, tubular and ellipsoidal) and volume, are shown in Fig. 2. More details are reported by Berthod et al. [21]. Every insert was filled with the same activity concentration and placed in a non-radioactive water background.
2. The same Anthropomorphic phantom already described above was prepared with different activity concentrations and scanned a second time.

Details of inserts, volumes and activity concentrations are collected in Table 2.

Percentage difference (Error (%)) between quantified activity and true activity was calculated to estimate the accuracy of quantification, using the following formula:

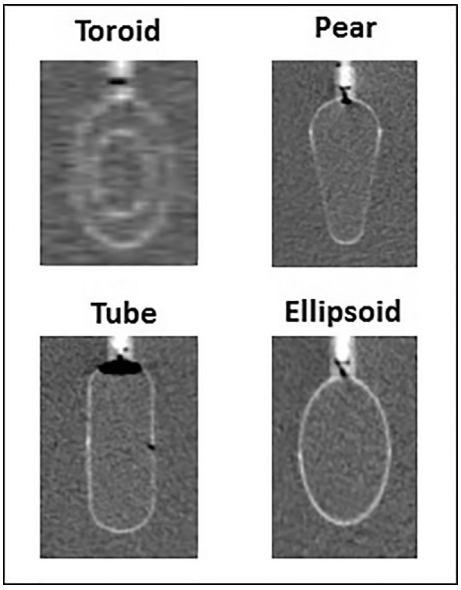

Fig. 2. Section of CT scan for different insert-shape of the Cylindrical phantom.

$$Error\ (\%) = \frac{Quantified\ activity - True\ activity}{True\ activity}{\cdot}100 \quad (4)$$

Quantified activity was empirically obtained measuring counts from the SPECT image and using Eq. (1) in case no PVC is applied, or Eq. (3) in case PVC is applied.

Finally, the "compactness" for each insert shape was quantitatively estimated using the parameter asphericity (ASP), defined by Apostolova et al. [22] as follows:

$$\boldsymbol{ASP} = 100{\cdot}(\sqrt[3]{\boldsymbol{H}} - 1)\boldsymbol{with}\ \boldsymbol{H} = \frac{1}{36\pi}{\cdot}\frac{\boldsymbol{S}^3}{\boldsymbol{V}^2} \quad (5)$$

where S and V are the surface and the volume of the insert, respectively. ASP measures the deviation of a particular non-spherical VOI from the shape of a sphere with the same equivalent volume. ASP was evaluated to investigate its influence on PVC.

3. Results

3.1. PHASE 1: determination of the recovery coefficient (RC)

The RCs for the two different phantoms were calculated using Eq. (2) and were plotted versus the volume of the insert (Fig. 3). The error bars in the plot show the value of uncertainty associated to the RCs,

Table 2
Description of phantoms used to test the partial volume effect curve. Each insert was named as his diameter (for example the Toroid with 26 mm of diameter as To26).

Phantom	Phantom Volume (ml)	Insert	Insert inner volume (ml)	Background activity concentration (MBq/ml)	Insert Activity concentration (MBq/ml)
Geometrical phantom	6713	To17a	2.8	No background	1.53
		To26	9.7		
		E22	5.5		
		E30	14.8		
		E38	28.5		
	6713	To17b	2.8		
		P38	29.2		
		P39a	30.1		
		P39b	31.2		
			0.2		
		Tu38a	28.6		
		Tu38b	28.8		
Anthropomorphic phantom 2	8153	Pancreas	92	0.03	0.99
		Right Kidney	142		0.82
		Left Kidney	142		0.81
		Spleen	156		1.10
		Liver	1470		0.53

estimated as previously described (section: 'Material and methods – *PHASE 1*: Determination of the Recovery Coefficients (RCs)').

To obtain the best fitting function to the RCs the functions in Eqs. (6) and (7) were used. In particular Eq. (6) was used for the RCs obtained with the spherical inserts, which are all in a range of volume affected by PVE. Eq. (7) was instead used for the anthropomorphic inserts, to obtain the convergence of the RC curve to 1 in case of the largest volumes.

$$RC = a \cdot e^{-b \cdot Volume} + c \quad (6)$$

$$RC = a \cdot e^{-b \cdot Volume} + 1 \quad (7)$$

where a, b and c are the fitting parameters, Volume and RC respectively the independent and dependent variables. Physical constraints for RC were set at 1 for the upper limit and 0 for the lower limit.

The Bravais-Pearson correlation coefficient (r) and the Root Mean Square Deviation (RMSD) were calculated to evaluate the quality of the fitting model. They are reported in Fig. 3.

3.2. PHASE 2: assessment of partial volume correction with RCs

To test the RC curves we used Eq. (4) to compare the discrepancy in the activity quantification in the case of PVC and in the case of no PVC. Activity in case of PVC was obtained applying Eq. (3), where the RC factor is extrapolated from the RC curve (Fig. 3) for the specific volume of the insert. In particular for the Geometrical phantom the curve obtained with the sphere phantom was used (Fig. 3a), instead for the Anthropomorphic phantom the curve obtained with the organs (Fig. 3b). Figs. 4 and 5 show the Error (%) for the two test phantoms (respectively Geometrical and Anthropomorphic phantoms).

Fig. 6 shows the Error (%) of PVC activity as a function of the ASP for the Geometrical inserts and the value of the Pearson correlation coefficient.

4. Discussion

At present activity quantification is one of the most critical step in dosimetry calculation, and PVE one of the most important source of error. PVE can produce a large bias in measured activity, especially for lesions and regions with a small volume [23].

The intention of this experiment was to generate a model to be applied easily in practice when activity correction for partial volume effect is desired. The method based on RC was chosen for its simplicity both in formulation and application. It can be employed in every institute by following the same procedure and, once the RC curve is well defined, it can be applied by using only the volume of the lesion or of the organ. The RC method was demonstrated by Tran-Gia et al. [24] to be the most accurate respect to others based on enlarged VOI, peak-ml and the fixed threshold. However, one of its limitations is that it does not take into account the spill-over from other regions. Algorithms that account for this were already proposed, as the GTM or the mMGM well described by Erlandsson et al. [25]. However these techniques are difficult to implement, and usually lead to noise-amplification or image artefacts [26]. Therefore a RC-based method may be preferred in

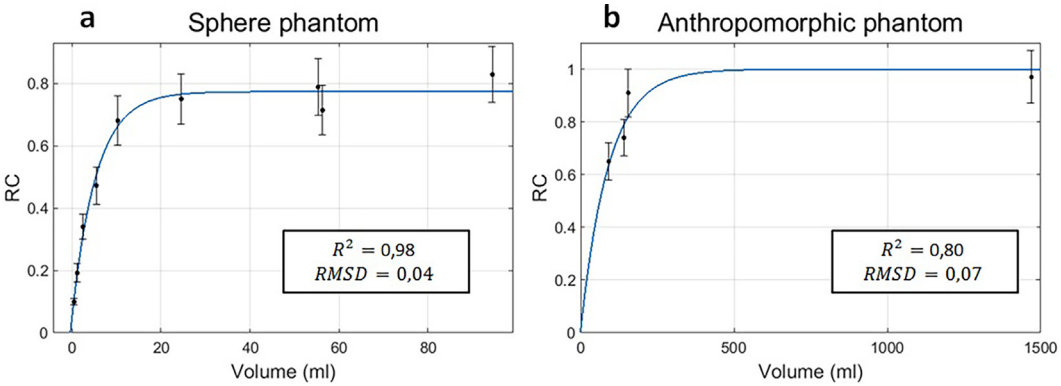

Fig. 3. RCs for the Sphere phantom (a) and Anthropomorphic phantom (b). The exponential RC curves and the R^2 and RMSD values are also reported in the graphs. Note for left kidney and right kidney only one RC point is distinguishable in the graph because of their similar value.

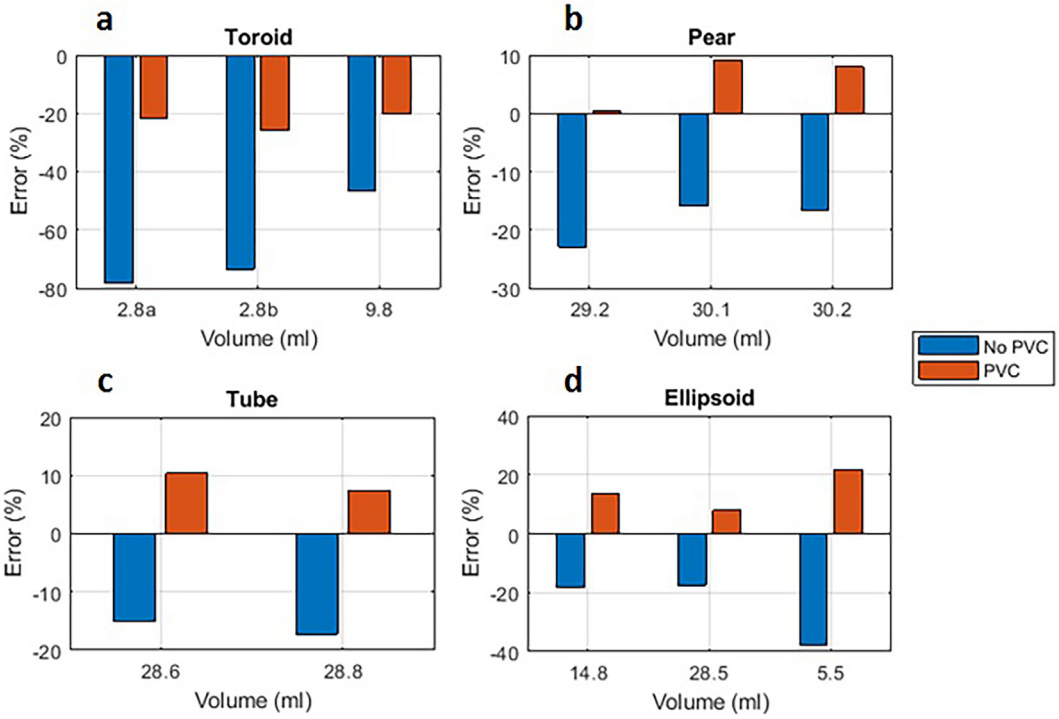

Fig. 4. Accuracy of the activity quantification for all inserts of Geometrical phantom, in case of no PVC and in case of PVC.

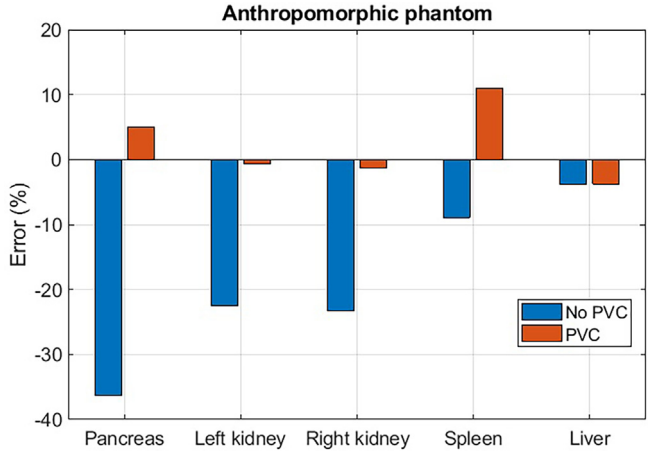

Fig. 5. Accuracy of activity quantification for inserts of Anthropomorphic phantom, in case of no PVC and in case of PVC.

clinics.

The choice to use two different phantoms for determination of the RC has been made considering the clinical applications. PVC is in fact applied to lesions and organs, which span a large interval of volumes, from the smallest lesions (in accordance with the spatial resolution limit) to the largest organ size (e.g.: liver). Lesions are generally not characterized by a specific shape and it's very difficult to find the most accurate RC for each lesion geometry. Lesions have the most different shapes and naturally show very dissimilar geometries from a sphere. It would be impossible to take into account experimentally all the occurring geometries in practice. For this reason in the current study authors considered the spherical geometry as representative for the category of the lesions when extrapolating the RC curve, and studied the influence of the asphericity on the RCs when testing the RC curve. In fact, the acquisition of additional phantoms with various geometrical shapes has permitted to evaluate errors that result from the spherical approximation. As regards organs, instead, we considered a single PVE model that includes all organs (i.e. a phantom containing all inserts was scanned). Although more accurate values of RC would be obtained if every single organ had been considered (i.e. by acquiring each organ separately), this method is easier for clinical practice and allows to perform only one phantom acquisition. A further acquisition of the anthropomorphic phantom has permitted to evaluate accuracy of quantification using this simplified modeling.

A marked improvement in the quantification of activity was observed when correction for PVE was adopted. Average percentage error over all inserts passed from −26% to 1.3% (from 26% to 10% as absolute values) when activities were corrected for PVE. However the improvement in activity quantification is not the same for all the inserts, but it mainly depends on the size and the shape of the VOI. Fig. 4a (Toroid) shows the correction of activity is not enough to compensate for the displaced counts because of PVE, while it involves an overestimation of activity in case of the other inserts (Fig. 4b–d). PVE correction decreased the discrepancy in activity quantification from −66% to −22% for the three toroids and from −19% to 4% for the other inserts. This highlights a clear dependence on the shape of the VOI and suggests that, using simple spherical inserts, activity quantification will be the less accurate the more the geometry differs from spherical shapes. Dependence on the shape of the VOI is quantitatively evaluated in Fig. 6, where Error (%) of PVC activity versus ASP (Eq. (7)) is plotted. A strong linear correlation between Error (%) and ASP was observed ($R^2 = 0.922$), as reported in the figure. Inserts with the same shape (vertically in the graph) showed higher value of Error (%) for larger volume (see the Toroids (To) and the Pears (P)), even if this trend was not observed for the Ellipsoid (E). A possible hypothesis to explain these results might be that relation between PVE and volume depends on the shape of the VOI (for example this relation is exponential in case of the spheres). Hence, the relation between Error (%) and volume will most likely be different depending on the shape of the insert. However, evaluation of this dependence is beyond the scope of this study, and could be investigated in a further study.

Similarly results for the Anthropomorphic phantom were shown in Fig. 5: the correction of activity is not the same for all the organs and it involves an overestimation in case of spleen. Using only one RC curve

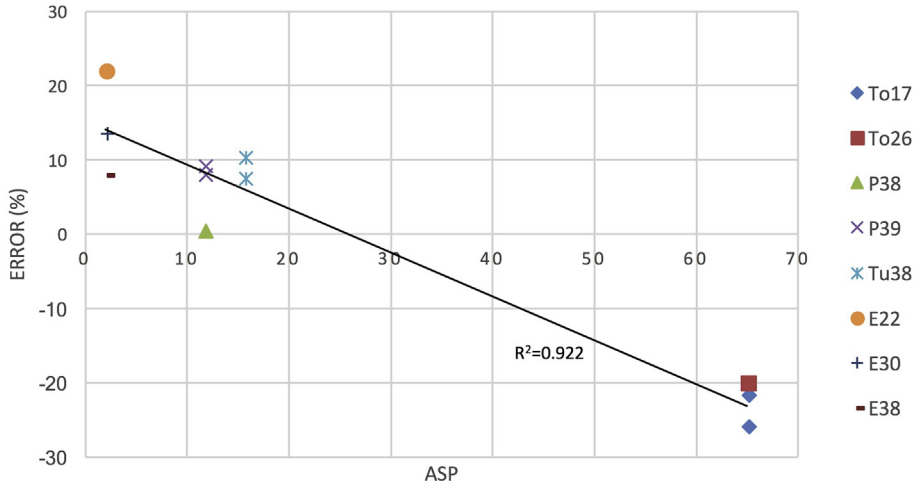

Fig. 6. Error(%) of PVC activity as a function of the ASP for the Geometrical phantom. The value of the Pearson correlation coefficient (R^2) is reported in the graph. A distinct data point format was used for inserts with different shape or equivalent diameter.

for all organs probably does not allow to take into account the differences in the PVE due to the different shape of the organs. Furthermore, the spill-over between the inserts of organs, which are closer to each other than the inserts placed in the 'geometrical phantom', probably involves an increased RC, especially for the spleen, which is close to the liver and the left kidney. Fig. 3 shows that RC value calculated for the spleen is far from RC curve fitted in the plot, and consequently compensation for PVE is too large. More accurate results would be most likely obtained using a curve for each organ, as also suggested by Robinson et al. [27], but it would be necessary to have different inserts for each organ, with various volumes. This is not easy in practice on a large scale at present. The use of a single RC curve for all the organs, however, provides an approximate improvement in the quantification of activity, though it has some limits.

The results of this work could be improved if the signal/background ratio were considered. As reported by Shyam et al. [28] the spill-in depends on this ratio and affects the PVE. However in this experiment this ratio was very low or almost absent in phantoms, and the contribution of spill-in was negligible.

More accurate estimates of RCs might be obtained with simulation study of whole imaging process. These algorithms require long time for the simulations, but if optimized this time could be reduced [29] and the algorithms more easily implemented in practice. Complete correction of activity quantification, nevertheless, is difficult to perform, especially in clinical practice [30]. One of the main limitation of this method based on physical measurements is the fact that not all anatomical structures can be well approximated by simple geometrical shapes, and anatomical variability between different patients is not easy to account for. The assumption that the VOI is placed into one homogeneous surrounding activity is not always valid, and signal/background ratio cannot be easily defined. In addition to this, PVE depends on the tomographic scanner, on the processing (image acquisition settings and reconstruction algorithms, scatter correction, VOI definition technique, ….) and on the measurement procedure. RC should be calculated individually for each scanner in all centres, but a standardized procedure to define these coefficients should be investigated.

5. Conclusion

This study has provided a practical method for PVC based on phantom measurements and on RC curve.

Although some approximations are inherent in this method, a marked improvement in the activity quantification was observed. The RCs can be easily estimated in each institute by following a standard procedure, or using more complex phantoms if higher accuracy is desired. The importance to calculate RCs for lesions and organs, and to characterize the RCs for different geometrical shapes are the main issues pointed out with this study.

References

[1] Mahase SS, Wernicke AG, Nori D, et al. Current and emerging roles of functional imaging in radiation therapy. Discovery Med 2015;19(104):203–11.
[2] Weber WA. Use of PET for monitoring cancer therapy and for predicting outcome. J Nucl Med 2005;46:983–95.
[3] Ljungberg M, Celler A, Konijnenberg MW, et al. MIRD Pamphlet No. 26: joint EANM/MIRD guidelines for quantitative 177Lu SPECT applied for dosimetry of radiopharmaceutical therapy. J Nucl Med 2016;57(1):151–62.
[4] Huizing DMV, de Wit-van der Veen V, Verheij M, et al. Dosimetry methods and clinical applications in peptide receptor radionuclide therapy for neuroendocrine tumours: a literature review. EJNMMI Res 2018;29 8(1):89.
[5] Grassi E, Fioroni F, Berenato S, et al. Effect of image registration on 3D absorbed dose calculations in ^{177}Lu-DOTATOC peptide receptor radionuclide therapy. Phys Med 2018;45:177–85.
[6] Dewaraja YK, Ljungberg M, Green AJ, et al. MIRD pamphlet No. 24: guidelines for quantitative 131I SPECT in dosimetry applications. J Nucl Med 2013;54(12):2182–8.
[7] Siegel JA, Thomas SR, Stubbs JB, et al. MIRD Pamphlet No. 16: techniques for quantitative radiopharmaceutical biodistribution data acquisition and analysis for use in human radiation dose estimates. J Nucl Med 1999;40:37S–61S.
[8] Shankar LK, Hoffman JM, Bacharach S, et al. Consensus recommendations for the use of 18F-FDG PET as an indicator of therapeutic response in patients in National Cancer Institute trials. J Nucl Med 2006;47:1059–66.
[9] Soret M, Bacharach SL, Buvat I. Partial-volume effect in PET tumor imaging. J Nucl Med 2007;48:932–45.
[10] Hoffmann EJ, Huang SC, Phelps ME. Quantitation in positron emission computed tomography: effect of object size. J Comput Assist Tomogr 1979;3(3):299–308.
[11] Dewaraja YK, Ljungberg M, Koral K. Monte Carlo evaluation of object shape. Eur J Nucl Med 2001;28:900–6.
[12] Mazzenga E, D'Errico V, D'Arienzo M, et al. Quantitative accuracy of 177Lu SPECT imaging for molecular radiotherapy. PLoS ONE 2017;12(8):e0182888.
[13] NEMA Standards Publication NU 2–2007, Performance measurements of positron emission tomographs; 2007. p. 26–33.
[14] Ogawa K, Harata Y, Ichihara, et al. A practical method for position-dependent Compton scatter correction in single photon emission CT. IEEE Trans Med Imaging 1991;10(3):408–12.
[15] Shcherbinin P, Piwowarska-Bilska H, Celler A, et al. Quantitative SPECT/CT reconstruction for 177-Lu and 177-Lu/90-Y targated radionuclide therapies. Phys Med Biol 2012;57:5733–47.
[16] Grassi E, Fioroni F, Mazzenga E, et al. Impact of a commercial 3D OSEM reconstruction algorithm on the 177Lu activity quantification of SPECT/CT imaging in a Molecular Radiotherapy trial. Radiol Diagn Imaging 2017;1(1):1–7.
[17] Uribe CF, Esquinas PL, Celler A, et al. Accurancy of 177Lu activity quantification in SPECT imaging: a phantom study. EIJNMMI Phys 2017;4(1):2.
[18] Deasy JO, Blanco AI, Clark VH. CERR: a computational environment for radiotherapy research. Med Phys 2003;30(5):979–85.
[19] Kessler RM, Ellis K, Eden M. Analysis of emission tomographic. J Comput Assist Tomogr 1984;8:514–22.
[20] Grassi E, Fioroni F, Ferri V, et al. Quantitative comparison between the commercial software STRATOS® by Philips and a homemade software for voxel-dosimetry in

radiopeptide therapy. Phys Med 2015 Feb;31(1):72–9.
[21] Berthod B, Marshall C, Evans M, et al. Evaluation of advanced automatic PET segmentation methods using nonspherical thin-wall inserts. Med Phys 2014;41(2):022502.
[22] Apostolova I, Steffen IG, Wedel F, et al. Asphericity of pretherapeutic tumour FDG uptake provides independent prognostic value in head-and-neck cancer. Eur Radiol 2014;24:2077–87.
[23] D'Arienzo M, Cozzella ML, Fazio A, et al. Quantitative ^{177}Lu SPECT imaging using advanced correction algorithms in non-reference geometry. Phys Med 2016;32(12):1745–52.
[24] Tran-Gia J, Lassmann M. Optimizing image quantification for Lu-177 SPECT/CT based on a 3D printed 2-compartment kidney phantom. J Nucl Med 2018;59(4):616–24.
[25] Erlandsson K, Buvat I, Pretorius PH, et al. A review of partial volume correction techniques for emission tomography and their applications in neurology, cardiology and oncology. Phys Med Biol 2012;57(21):R119–59.
[26] Thomas BA, Improved brain PET quantification using partial volume correction techniques. Doctoral Thesis, 2012. Retrieved from UCL Discovery.
[27] Robinson AP, Tipping J, Cullen DM, et al. Organ-specific SPECT activity calibration using 3D printed phantoms for molecular radiotherapy dosimetry. EJNMMI Phys 2016;3(1):12.
[28] Shyam M, Thiruvenkatasamy D. A recovery coefficient method for partial volume correction. Ann Nucl Med 2009;23(4):341–8.
[29] Lin H, Ayan A, Zhai H. A quantitative evaluation of velocity AI deformable image registration. Med Phys 2010;37.
[30] Ritt P, Vija H, Hornegger J, et al. Absolute quantification in SPECT. Eur J Nucl Med Mol Imaging 2011;38(Suppl. 1):S69–77.